ChemComm

COMMUNICATION

View Article Online
View Journal | View Issue

Cite this: *Chem. Commun.*, 2017, 53, 9125

Received 8th June 2017,
Accepted 17th July 2017

DOI: 10.1039/c7cc04440b

rsc.li/chemcomm

Catalytic role of vacancy diffusion in ceria supported atomic gold catalyst†

Zhong-Kang Han,[ab] Yang-Gang Wang*[c] and Yi Gao*[ad]

Dynamics of intrinsic defects are considered fundamental in the chemistry of reducible oxides, and their effect on catalytic reactions have been rarely reported. Herein, we propose a new O_v diffusion assisted Langmuir–Hinshelwood mechanism for CO oxidation, which may largely account for the origin of high reactivity of supported atomic gold catalysts.

The prominent redox properties have enabled the use of reducible oxides, such as titania (TiO_2) and ceria (CeO_2), as important support materials or catalysts in heterogeneous catalysis.[1–6] The intrinsic defects such as oxygen vacancies (O_vs), interstitials and surface steps, which ubiquitously exist in reducible oxides, have been extensively examined in literature.[7–15] However, few studies are devoted to discussing their effect on the realistic catalytic reactions. This is primarily because of the complexity of the systems with multiple local minima with respect to the sites on which the excess electrons-driving the Ce^{4+} ($4f^0$) to Ce^{3+} ($4f^1$) reduction-localize.[8,9,16] In this study, we chose ceria supported Au adatoms (monomer and dimer) as typical examples and carried out thorough density-functional theory investigations to explore the dynamics of intrinsic defects accompanying the redistribution of the 4f localized electronic states, and illustrated their key role in catalysing CO oxidation processes.

Ceria-supported gold catalysis has attracted extensive interest in the past decade due to its excellent performance in three-way catalysis, low temperature water–gas shift reaction, dehydrogenation reaction, and other catalytic applications.[17–20] The high reactivity is generally attributed to the strong metal support interaction between ceria and gold particles.[21,22] In particular, O_vs, the most common defects in ceria, can engender excess charges to the system, which not only enhance the binding of gold particles, but also adjust the oxidation state of gold particles.[5,23] However, controversies still exist concerning the role of O_v in gold catalysis. First, on one hand, most studies reported that gold cluster preferentially occupied the surface O_v of the support.[4,24–27] On the other hand, recent studies showed that the subsurface O_v was more stable than the surface O_v and was the dominant species on reduced ceria surface.[28,29] Second, extensive studies have shown that the presence of oxygen vacancy in ceria support can significantly increase the activity of gold catalysis.[4,30–33] However, Weststrate *et al.*[27] recently showed that highly dispersed gold adatoms on reduced ceria seem to bind molecular CO more weakly than oxidized ceria. Camellone *et al.*[5] demonstrated that the oxygen vacancy provides an inhibiting effect on the activity of supported gold catalysts but this effect weakens as the cluster size of gold increases. Therefore, an in-depth understanding of the interplay between gold adatoms and near-surface O_vs is of fundamental importance to explore the nature of high reactivity of supported gold catalysts.

The calculations have been performed within the framework of DFT with generalized gradient approximation using the VASP code.[34,35] The DFT+*U* methodology was used in this study, which has been extensively utilized for ceria in literature.[9,16,23,36–38] Previous studies indicated that multiple self-consistent solutions exist, corresponding to different occupations of the *m* projections associated with the f-shell to which the *U* parameter is applied.[39,40] However, in this study, the used Davidson-block iteration scheme with random initialization of the orbitals, for which the most extensive tests have been performed, is considerably robust[41] (see calculation details in ESI†).

To validate our methodology, the types and distributions of O_vs in the bare ceria slab (Fig. S1, S2 and Tables S1, S2, ESI†) were further examined. The most stable configurations for single surface O_v (SSV) and single subsurface O_v (SSSV) on CeO_2(111) surface contain two excess electrons both located at the next-nearest neighbour cerium positions relative to the

[a] *Division of Interfacial Water and Key Laboratory of Interfacial Physics and Technology, Shanghai Institute of Applied Physics, Chinese Academy of Sciences, Shanghai, 201800 China. E-mail: gaoyi@sinap.ac.cn*
[b] *University of Chinese Academy of Sciences, Beijing, 100049 China*
[c] *Fritz-Haber-Institut der Max-Planck-Gesellschaft, Berlin-Dahlem, 14195 Germany. E-mail: wangygtccl@gmail.com*
[d] *Shanghai Science Research Center, Chinese Academy of Sciences, Shanghai, 201204 China*

† Electronic supplementary information (ESI) available: Multiple localization of the excesses 4f electrons. See DOI: 10.1039/c7cc04440b

vacancy site itself. The calculated O_v formation energy of SSSV (1.91 eV) is 0.19 eV lower than that of SSV (2.10 eV), suggesting that SSSV is energetically more stable than SSV (Table S1, ESI†). This is quantitatively consistent with previous calculations (0.18 eV).[9] In addition, our further examinations indicate that the vacancies tend to separate up to a distance equal to twice of the (1 × 1) surface lattice parameter (Fig. S1 and Table S1, ESI†), *i.e.*, the third-nearest neighbour in the subsurface layer, to form oxygen vacancy pairs, which is consistent with the recent experiments and calculations.[28,29]

Prior to investigating the reaction mechanism of CO oxidation, we consider the interplay between gold adatoms and O_vs (Fig. S3–S5 and Tables S3, S4, ESI†), which is generally believed to be important to promote the catalytic activity of gold. For a gold monomer on CeO_2(111) support with one O_v (SSV or SSSV), the most stable configurations are shown in Fig. S4a and c, ESI.† It is found that the gold monomer occupied SSV is much more stable than the SSSV with gold monomer binding to the surface oxygen, though SSSV is more stable without the presence of the gold monomer. Specifically, we find that the SSSV only needs to experience a small energy barrier of 0.27 eV to hop up from subsurface to surface site in the presence of a single gold adatom. During the hopping process, the number of excess electrons at Ce sites is reduced from 3 to 1, suggesting that the charge state of gold adatom changes from +1 to −1 by attaining two excess electrons. These results are consistent with previous calculations.[4,5,12,23,42,43]

We further introduce another Au atom and an extra O_v into the system to explore the effect of high concentration of vacancies on the behaviour of gold cluster. The most stable configurations for Au_2@CeO_2(111)-SS-SS, Au_2@CeO_2(111)-SS-S and Au_2@CeO_2(111)-S-S (SS means subsurface O_v and S means surface O_v) are listed in Fig. 1. We find an interesting reconstruction process of Au dimer in the presence of O_v pair. Initially, Au dimer is put on the surface bridged oxygen ions and the two O_v are located in the subsurface layer. The system only has 4 excess electrons corresponding to the two O_v and the charge state of Au dimer is roughly estimated to be neutral. It is shown that one of the two O_v could easily hop up from the subsurface to the surface and be filled immediately by one Au atom. This process only needs an extremely small energy barrier of 0.04 eV (TS1 in Fig. 1). Simultaneously, it will reduce the oxidation state of the gold atom, which fills into the surface O_v, from 0 to −1 but the other Au is oxidized from 0 to +1. Further hopping of the other O_v with a barrier of 0.88 eV (see TS2 in Fig. 1) is relatively difficult, partially due to the strong Coulombic repulsion of two Au-ions when both the O_v locate on the surface. These results strongly imply that under realistic conditions, not all the excess charges from O_vs can have an impact on the gold particles due to the thermodynamically unfavorable Coulombic repulsion. Compared to the gold monomer, the presence of Au dimer cluster seems to improve the stability of subsurface O_v. The energy difference for three distributions of O_v shown in Fig. 1 is less than 0.2 eV.

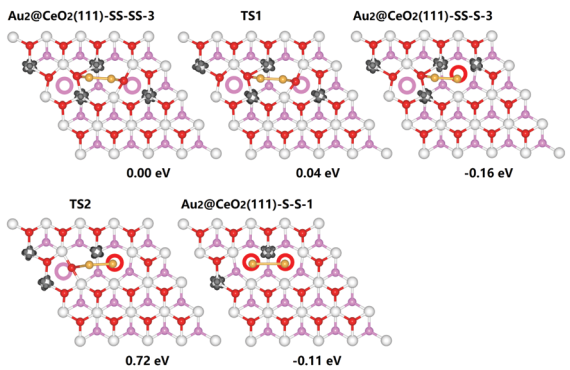

Fig. 1 Calculated path and corresponding energetics for the migration of O_v on Au_2@CeO_2(111)-SS(S)-SS(S)-*N*. In CeO_2(111)-SS(S)-SS(S)-*N*, SS(S) means subsurface (surface) O_v and *N* means they are in the *n*th nearest neighbour position. The spin density isosurface is shown in dark area. Cerium, surface oxygen, and subsurface oxygen atoms are depicted in white, red, and pink, respectively. Open circles represent oxygen vacancies. For clarity, only the first O–Ce–O trilayer (TL) is shown.

Based on the most stable configurations of ceria-supported Au adatoms, we now consider the reactivity of CO oxidation to explore the potential effect of oxygen vacancy-metal interplay on the catalytic reactivity of reducible oxide supported metal particles. For Au monomer in O_v, the adsorption of CO is very weak (E_{ad} = −0.16 eV) due to the full-occupied 6s orbitals of negatively charged Au, consistent with previous studies.[5] Therefore, next, we only consider the reaction mechanisms of CO oxidation on ceria-supported gold dimer, where one O_v locates at the subsurface layer and the other locates at the surface layer. We find a novel Langmuir–Hinshelwood (LH) mechanism assisted by the hopping of oxygen vacancy between the surface layer and subsurface layer, which exhibits significantly higher reactivity than the traditional LH mechanism. Note that the Mars–van Krevelen Mechanism was also tested for existence but did not prove to be prevalent in this study (Fig. S6, ESI†).

In the traditional L–H mechanism (see Fig. 2a), reaction only involves CO reacting with the adsorbed O_2 species and the O_vs are not allowed to diffuse during the entire process. Initially, CO is adsorbed on the gold dimer with adsorption energy of −1.58 eV but O_2 molecule only weakly binds to one Au atom. The adsorption energy is −0.31 eV and the bond length of adsorbed O_2 is 1.24 Å, close to 1.23 Å in the gas phase, suggesting a physisorption of O_2. Next, CO and O_2 move towards each other, forming an O–C–O–O* complex. This step experiences a barrier of 0.68 eV and is slightly endothermic by 0.12 eV. Subsequent formation of a gas-phase CO_2 is highly exothermic (−2.17 eV). The residual O* can directly react with an additional gas-phase CO to form CO_2 molecule, completing the reaction cycle.

In contrast, Fig. 2b shows a dynamic reaction mechanism of CO oxidation assisted by the oxygen vacancy diffusion. CO initially adsorbs to the Au dimer with high adsorption energy of −1.58 eV. Distinctly different from the traditional L–H mechanism, O_2 adsorption is significantly enhanced by 0.31 eV, when the surface O_v diffuses into the subsurface by overcoming a small barrier of 0.29 eV. The bond length of the adsorbed O_2 is increased to 1.33 Å, indicating the formation of superoxide species (O_2–). After that, the adsorbed CO and O_2 only need to experience a barrier of 0.15 eV to form an O–C–O–O* complex. Subsequent reactions

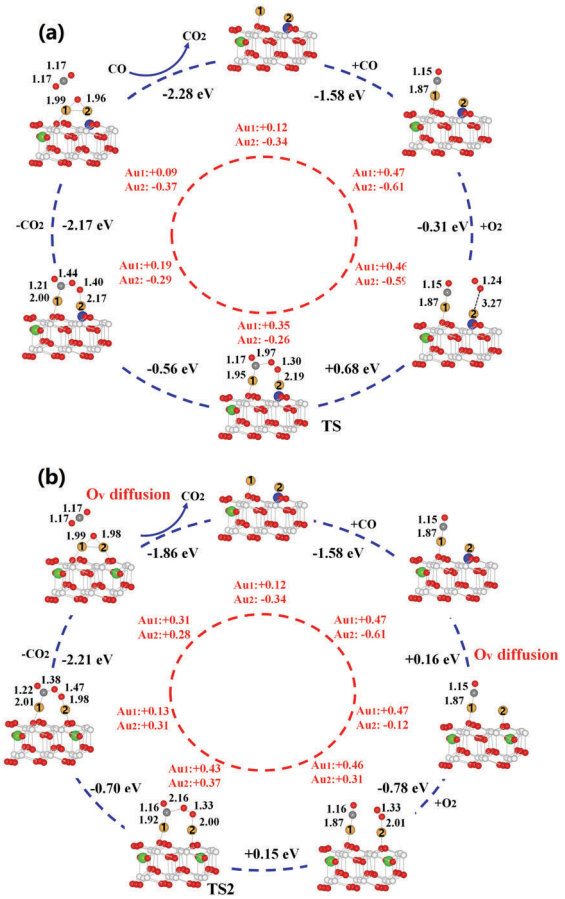

Fig. 2 Catalytic cycle and corresponding charge cycle for the oxidation of CO catalysed by Au_2@CeO_2(111) *via* the traditional (a) and novel (b) L–H reaction mechanisms. The charges corresponding to gold adatoms are labeled as 1 and 2, respectively. Colour schemes: Au, gold; Ce, white; surface O, red; subsurface O, pink; surface O_v, blue; subsurface O_v, green; C, grey.

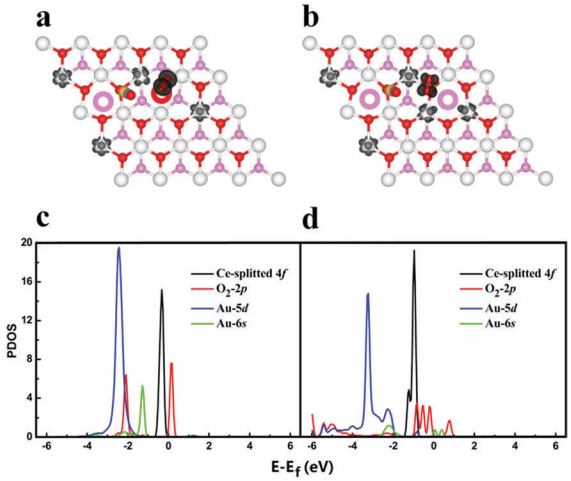

Fig. 3 Co-adsorption of CO and O_2 on Au_2@CeO_2(111)-SS-S-3 (a) and Au_2@CeO_2(111)-SS-SS-3 (b) and their projected density of state (c) and (d), respectively. The colour schemes are same with Fig. 1.

such as CO_2 formation and the removal of O by an additional CO are similar to the traditional L–H mechanism. After all the adsorbed species are removed, one of the subsurface oxygen will hop back to the surface layer, completing the catalytic cycle. Overall, O_v diffusion enhances the adsorption of O_2 molecule by 0.31 eV, lowers the energy barrier of rate-determining step by 0.53 eV and stabilizes the intermediate complex by 0.98 eV. After the catalytic cycle is completed, one O_v will hop back to the surface layer, charging the Au cluster and stabilizing it. Therefore, the proposed O_v diffusion assisted L–H mechanism is expected to exhibit much higher reactivity than the traditional mechanism, which may largely contribute to the high reactivity of ceria supported gold particles at low temperatures.

To understand the nature of the enhancement effect from O_v diffusion, we first monitor the charge state of Au dimer during the catalytic cycle. It is shown that the migration of O_v from surface to subsurface leads to the re-oxidation of negatively charged gold adatom, which initially occupies the O_v site, implying that the strong interplay between ceria support and the gold adatoms may occur upon O_v diffusion. We thus further analyse the change of spin density isosurface and the projected density of states (PDOS) during the O_v diffusion processes, as shown in Fig. 3. In Fig. 3a and b, it is found that one additional 4f electron is localized on a Ce atom when the surface O_v migrates to the subsurface, indicating electron transfer from gold atom to ceria. This is further confirmed by the increase of 4f states in Fig. 3c and d. Before the diffusion, the energy levels of unoccupied O_2 $2\pi^*$ states are higher than both saturated Au 6s states and occupied 4f states, and the O_2 is thus not able to be activated. When the O_v migrates into the subsurface, the occupied Au 6s states become strongly correlated with the lattice O 2p (valence band) and as a result, the energy level of 6s gets lifted, which can release excess electrons into the Ce 4f states and unoccupied O_2 $2\pi^*$ states. Moreover, the resultant Au 6s empty states can interact with the occupied O_2 2p states, leading to a down shift of these states and stabilizing the adsorbed O_2. In other words, the O_v diffusion essentially activates the Au 6s states so that they can correlate well with the frontier states of adsorbed intermediates such as O_2* and O–C–O–O* complex and activate them by charge transfer.

In summary, we have presented a thorough understanding of charge distributions resulting from O_vs and proposed a newly dynamic L–H reaction mechanism for CO oxidation on ceria-supported Au dimer. The diffusion of O_v between the surface and subsurface layer is shown to promote the reactivity of CO oxidation during the catalytic cycle and stabilize the Au dimer after the cycle is completed. In general, this study strongly suggests that the interplay between metal particle and the intrinsic defect of the support is vital in understating the origin of high reactivity of oxide supported gold catalysis.

This study is supported by the National Natural Science Foundation of China (11574340), and the CAS-Shanghai Science Research Center (Grant No. CAS-SSRC-YJ-2015-01). Y. G. W. thanks the financial supported by Alexander von Humboldt Foundation. The authors also thank the Special Program for Applied Research on Super Computation of the NSFC-Guangdong Joint Fund (the second phase) under Grant No. U1501501. The computational resources utilized in this research were provided by Shanghai

Supercomputer Center, National Supercomputer Centers in Tianjin, Shenzhen.

References

1 M. Dresselhaus and I. Thomas, *Nature*, 2001, **414**, 332–337.
2 Q. Fu, H. Saltsburg and M. Flytzani-Stephanopoulos, *Science*, 2003, **301**, 935–938.
3 G. Deluga, J. Salge, L. Schmidt and X. Verykios, *Science*, 2004, **303**, 993–997.
4 Z.-P. Liu, S. J. Jenkins and D. A. King, *Phys. Rev. Lett.*, 2005, **94**, 196102.
5 M. F. Camellone and S. Fabris, *J. Am. Chem. Soc.*, 2009, **131**, 10473–10483.
6 Y.-G. Wang, D. C. Cantu, M.-S. Lee, J. Li, V.-A. Glezakou and R. Rousseau, *J. Am. Chem. Soc.*, 2016, **138**, 10467–10476.
7 C. Zhang, A. Michaelides, D. A. King and S. J. Jenkins, *Phys. Rev. B: Condens. Matter Mater. Phys.*, 2009, **79**, 075433.
8 M. V. Ganduglia-Pirovano, J. L. Da Silva and J. Sauer, *Phys. Rev. Lett.*, 2009, **102**, 026101.
9 H.-Y. Li, H.-F. Wang, X.-Q. Gong, Y.-L. Guo, Y. Guo, G. Lu and P. Hu, *Phys. Rev. B: Condens. Matter Mater. Phys.*, 2009, **79**, 193401.
10 Y.-G. Wang, D. Mei, J. Li and R. Rousseau, *J. Phys. Chem. C*, 2013, **117**, 23082–23089.
11 Y.-G. Wang, Y. Yoon, V.-A. Glezakou, J. Li and R. Rousseau, *J. Am. Chem. Soc.*, 2013, **135**, 10673–10683.
12 Z.-K. Han and Y. Gao, *Nanoscale*, 2015, **7**, 308–316.
13 M. Moser, V. Paunovic, Z. Guo, L. Szentmiklosi, M. G. Hevia, M. Higham, N. Lopez, D. Teschner and J. Perez-Ramirez, *Chem. Sci.*, 2016, **7**, 2996–3005.
14 D. H. Barrett, M. S. Scurrell, C. B. Rodella, B. Diaz, D. G. Billing and P. J. Franklyn, *Chem. Sci.*, 2016, **7**, 6815–6823.
15 Z. K. Han and Y. Gao, *Chem. – Eur. J.*, 2016, **22**, 2092–2099.
16 H.-Y. Li, H.-F. Wang, Y.-L. Guo, G.-Z. Lu and P. Hu, *Chem. Commun.*, 2011, **47**, 6105–6107.
17 D. Andreeva, R. Nedyalkova, L. Ilieva and M. Abrashev, *Appl. Catal., A*, 2003, **246**, 29–38.
18 C. Zhang, A. Michaelides and S. J. Jenkins, *Phys. Chem. Chem. Phys.*, 2011, **13**, 22–33.
19 M. Wang, F. Wang, J. Ma, M. Li, Z. Zhang, Y. Wang, X. Zhang and J. Xu, *Chem. Commun.*, 2014, **50**, 292–294.
20 X. J. Jin, K. Taniguchi, K. Yamaguchi and N. Mizuno, *Chem. Sci.*, 2016, **7**, 5371–5383.
21 D. Widmann and R. J. Behm, *Angew. Chem., Int. Ed.*, 2011, **50**, 10241–10245.
22 D. Widmann and R. J. Behm, *Acc. Chem. Res.*, 2014, **47**, 740–749.
23 C. Zhang, A. Michaelides, D. A. King and S. J. Jenkins, *J. Am. Chem. Soc.*, 2010, **132**, 2175–2182.
24 T. Akita, M. Okumura, K. Tanaka, M. Kohyama and M. Haruta, *J. Mater. Sci.*, 2005, **40**, 3101–3106.
25 J. A. Rodriguez, P. Liu, J. Hrbek, J. Evans and M. Perez, *Angew. Chem., Int. Ed.*, 2007, **119**, 1351–1354.
26 J.-L. Lu, H.-J. Gao, S. Shaikhutdinov and H.-J. Freund, *Catal. Lett.*, 2007, **114**, 8–16.
27 C. Weststrate, R. Westerstrom, E. Lundgren, A. Mikkelsen, J. N. Andersen and A. Resta, *J. Phys. Chem. C*, 2008, **113**, 724–728.
28 S. Torbrügge, M. Reichling, A. Ishiyama, S. Morita and O. Custance, *Phys. Rev. Lett.*, 2007, **99**, 056101.
29 G. E. Murgida and M. V. Ganduglia-Pirovano, *Phys. Rev. Lett.*, 2013, **110**, 246101.
30 T. Tabakova, F. Boccuzzi, M. Manzoli and D. Andreeva, *Appl. Catal., A*, 2003, **252**, 385–397.
31 J. Rodriguez, M. Perez, J. Evans, G. Liu and J. Hrbek, *J. Chem. Phys.*, 2005, **122**, 241101.
32 A. Lindblad, R. Fink, H. Bergersen, M. Lundwall, T. Rander, R. Feifel, G. Öhrwall, M. Tchaplyguine, U. Hergenhahn and S. Svensson, *J. Chem. Phys.*, 2005, **123**, 211101.
33 R. Burch, *Phys. Chem. Chem. Phys.*, 2006, **8**, 5483–5500.
34 J. P. Perdew, K. Burke and M. Ernzerhof, *Phys. Rev. Lett.*, 1996, **77**, 3865.
35 G. Kresse and J. Furthmüller, *Phys. Rev. B: Condens. Matter Mater. Phys.*, 1996, **54**, 11169.
36 F. Esch, S. Fabris, L. Zhou, T. Montini, C. Africh, P. Fornasiero, G. Comelli and R. Rosei, *Science*, 2005, **309**, 752–755.
37 M. Nolan, S. C. Parker and G. W. Watson, *Surf. Sci.*, 2005, **595**, 223–232.
38 M. Nolan, J. E. Fearon and G. W. Watson, *Solid State Ionics*, 2006, **177**, 3069–3074.
39 B. Meredig, A. Thompson, H. Hansen, C. Wolverton and A. Van, de Walle, *Phys. Rev. B: Condens. Matter Mater. Phys.*, 2010, **82**, 195128.
40 J. Rabone and M. Krack, *Comput. Mater. Sci.*, 2013, **71**, 157–164.
41 G. E. Murgida, V. Ferrari, M. V. Ganduglia-Pirovano and A. M. Lois, *Phys. Rev. B: Condens. Matter Mater. Phys.*, 2014, **90**, 115120.
42 Y. Pan, N. Nilius, H.-J. Freund, J. Paier, C. Penschke and J. Sauer, *Phys. Rev. Lett.*, 2013, **111**, 206101.
43 M. a. M. Branda, N. C. Hernández, J. F. Sanz and F. Illas, *J. Phys. Chem. C*, 2010, **114**, 1934–1941.